

Landau model for the elastic properties of the ferroelastic crystal $\text{Rb}_4\text{LiH}_3(\text{SO}_4)_4$.

G. Quirion, W. Wu†, J. Rideout

Department of Physics and Physical Oceanography,

Memorial University, St. John's, Newfoundland, Canada, A1B 3X7

† *Department of Physics, University of Toronto, Toronto, Ontario, Canada*

B. Mróz

Institute of Physics, Adam Mickiewicz University, Poznan, Poland

(Dated: December 23, 2021)

We report a detailed investigation of the elastic properties of $\text{Rb}_4\text{LiH}_3(\text{SO}_4)_4$ measured as a function of temperature and pressure. $\text{Rb}_4\text{LiH}_3(\text{SO}_4)_4$ is known to show a $4 \rightarrow 2$ ferroelastic phase transition at $T_c = 134$ K. In order to clarify the nature of the order parameter associated with that structural transition, we compare our finding to two distinct phenomenological Landau models. The coupling parameters of both models are all determined using the temperature dependence of the strain tensor, as well as the pressure dependence $dT_c/dP = 19.1 \pm 0.2$ K/kbar, prior to the calculation of the elastic constants. Our comparison indicates that the ferroelastic transition in $\text{Rb}_4\text{LiH}_3(\text{SO}_4)_4$ is fully consistent (within a few percent) with the predictions of a pseudo-proper model, showing at the same time that the primary mechanism leading to the phase transition is not driven by strains. Our analysis also refutes the idea that $\text{Rb}_4\text{LiH}_3(\text{SO}_4)_4$ is the first ferroelastic compound showing incomplete softening, of the effective soft acoustic mode C_{soft} , at T_c .

PACS numbers:

I. INTRODUCTION

Over the years, there has been a series of controversies regarding the properties of the ferroelastic compound $\text{Rb}_4\text{LiH}_3(\text{SO}_4)_4$. Initially designated as $\text{LiRb}_5(\text{SO}_4)_2 \cdot 1.5\text{H}_2\text{SO}_4$ ^{1,2,3,4}, subsequent chemical analysis revealed that $\text{Rb}_4\text{LiH}_3(\text{SO}_4)_4$ is the proper description. It was also suggested that $\text{Rb}_4\text{LiH}_3(\text{SO}_4)_4$ belongs to the $4mm$ point group in the paraelastic phase at ambient temperature. Consequently, a $4mm \rightarrow 2mm$ symmetry change, associated with a ferroelastic phase transition at 134 K, was assumed^{5,6}. Additional X-ray⁷ and neutron diffraction⁸ measurements finally established that the proper group-subgroup symmetry change is actually $4 \rightarrow 2$. Based on this new phase sequence, the elastic properties of $\text{Rb}_4\text{LiH}_3(\text{SO}_4)_4$ have been revisited using Brillouin scattering⁹ and ultrasonic¹⁰ measurements. Both experimental approaches now confirmed that the effective elastic constant $(C_{11} - C_{12})/2$ softens as the temperature is reduced to T_c , which is perfectly compatible with a $4 \rightarrow 2$ phase transition. Nonetheless, in order to explain their respective findings, each group proposed models which are fundamentally different. On the one hand, the ultrasonic measurements¹⁰, which show a sudden drop at T_c in the velocity of longitudinal modes propagating along $[100]$ and $[001]$, are interpreted within the framework of a pseudo-proper ferroelastic model. Consequently, the authors assume that the order parameter is not one of the strains or a combination of strain components. However, in that case the order parameter must at least exhibit the same symmetry as the strain $(e_1 - e_2)$ or e_6 ¹¹. On the other hand, Mróz et al.⁹ claim that $\text{Rb}_4\text{LiH}_3(\text{SO}_4)_4$ shows incomplete softening at T_c and proposed a model which they claim is consistent

with that observation. In their paper, $\text{Rb}_4\text{LiH}_3(\text{SO}_4)_4$ is described as a proper ferroelastic compound where the strain combination $e_{soft} = \alpha_1 (e_1 - e_2) + \alpha_6 e_6$ acts as the order parameter. Incomplete softening in ferroelastic crystals is not a common phenomena, but it has previously been observed in BiVO_4 ¹². In that case, the softening is mediated by the coupling between optical and acoustical modes. Considering that the model proposed by Mróz et al.⁹ includes no such coupling term, we believe that their conclusion regarding the soft mode $\text{Rb}_4\text{LiH}_3(\text{SO}_4)_4$ requires further investigation. Thus, in order to clarify the nature of the ferroelastic transition, as well as, to validate or refute the possibility of incomplete softening in $\text{Rb}_4\text{LiH}_3(\text{SO}_4)_4$, we present a detailed investigation of the elastic properties of $\text{Rb}_4\text{LiH}_3(\text{SO}_4)_4$ as a function of temperature and pressure. We also compare the predictions of a proper and a pseudo-proper ferroelastic models in order to ascertain the character of the ferroelastic transition in $\text{Rb}_4\text{LiH}_3(\text{SO}_4)_4$.

II. EXPERIMENT

The $\text{Rb}_4\text{LiH}_3(\text{SO}_4)_4$ crystal was grown by the Crystal Physics Laboratory of the Institute of Physics at Mickiewicz University, Poland⁹. For the ultrasonic investigation, several samples in the form of cubes of about $3 \times 3 \times 3$ mm³ were used to measure the sound velocity along different crystallographic directions. Longitudinal and transversal waves were generated and detected using 30 MHz lithium niobate transducers mounted on one face of the crystal. The relative variations in the sound velocity ($\Delta V/V$) were obtained using a high-resolution pulsed acoustic interferometer as a function of temperature and

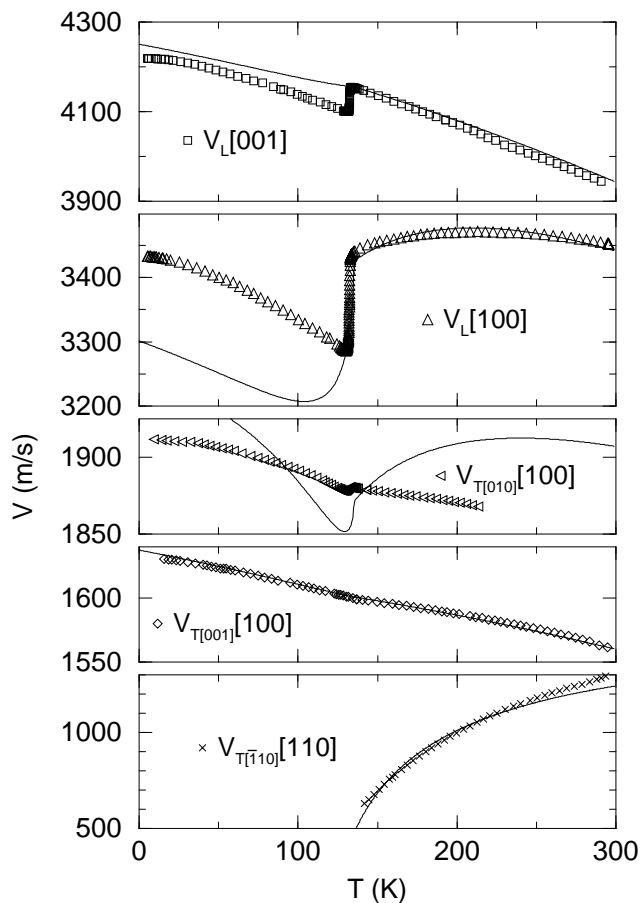


FIG. 1: Temperature dependence of the sound velocity of longitudinal (L) and transversal (T) modes measured along the principal crystallographic directions of $\text{Rb}_4\text{LiH}_3(\text{SO}_4)_4$. The experimental results are represented by open symbols while the continuous lines correspond to predictions derived from the pseudo-proper ferroelastic model presented in the Appendix.

pressure. For measurements realized at high pressure, the transducer-sample assemblage was inserted in a Cu-Be pressure cell filled with a 3-Methyl-1-butanol fluid acting as the pressure-transmitting medium. A small wire of Lead mounted close to the sample was used during the experiments to determine the actual pressure at different temperatures.

III. EXPERIMENTAL RESULTS

In this paper, the labels L and T are used to identify longitudinal and transverse modes, respectively. In addition, the Miller index adjacent to the label T gives the polarization of the mode while the other index corresponds to the direction of propagation. For example, $V_{T[001][100]}$ stands for the velocity of transverse wave propagating along the crystallographic direction [100] with its polarization along [001]. Using that notation, we present in

Fig. 1 and Fig. 2 our high resolution sound velocity results obtained for $\text{Rb}_4\text{LiH}_3(\text{SO}_4)_4$ as a function of temperature and pressure using modes propagating along the principal axes. In these figures, the experimental results are represented by open symbols while the continuous lines correspond to predictions derived from the pseudo-proper ferroelastic model presented in the Appendix VII B. Let first point out that our results are very consistent with previous studies^{9,10} realized as a function of temperature. As for the Brillouin scattering measurements⁹, the results presented in Fig. 1 indicate that the largest softening is observed for transverse modes propagating along [110] with a $[\bar{1}10]$ polarization ($V_{T[\bar{1}10][110]}$). In addition, our high resolution measurements show how the other modes change in the vicinity of the ferroelastic transition ($T_c = 132.8 \text{ K}$). In particular, we note that the velocity of longitudinal modes presented in Fig. 1 drop by a few percent at T_c . This observation is also consistent with previous ultrasonic measurements¹⁰. Our investigation is complemented with the first measurements realized as a function of pressure which we presented in Fig. 2. At ambient temperature, the data indicate a phase transition at a pressure of $P_c = 8.6 \pm 0.2 \text{ kbar}$. Considering that the observed anomalies on the elastic modes at T_c and P_c are very similar, we can assume that the transition observed at $P_c = 8.6 \pm 0.2 \text{ kbar}$ corresponds to a $4 \rightarrow 2$ ferroelastic structural transformation. To determine the pressure dependence of the critical temperature, we have carried out a series of sound velocity measurements as a function of temperature at different pressures. The results presented in Fig. 3 have been obtained using longitudinal waves propagating along the z-axis. From these measurements, we find that the ferroelastic transition temperature increases at a rate of $dT_c/dP = 19.1 \pm 0.2 \text{ K/kbar}$ with pressure (see inset of Fig. 3).

IV. DATA ANALYSIS

The results presented in Fig. 3 show that the temperature dependence just below the critical temperature changes significantly between ambient pressure and a moderate pressure of $P = 1.5 \text{ kbar}$. We believe that this might be an indication that the observed temperature dependence in the ferroelastic state is not purely intrinsic. One of the characteristic of ferroelastic compounds is that structural domains appear in the ferroelastic phase. Moreover for soft ferroelastic materials, it is possible to switch the orientation of these domains by applying an uniaxial stress. In the case of $\text{Rb}_4\text{LiH}_3(\text{SO}_4)_4$, the domains have been observed⁸ and consist of two mutually perpendicular walls. Considering that the pressure is not perfectly isotropic in pressure cell, the unusual behavior of the velocity close to T_c might be associated with a modification of the domain structure with increasing pressure. Consequently, before attempting to analyze any results in the ferroelastic phase, it is crucial to de-

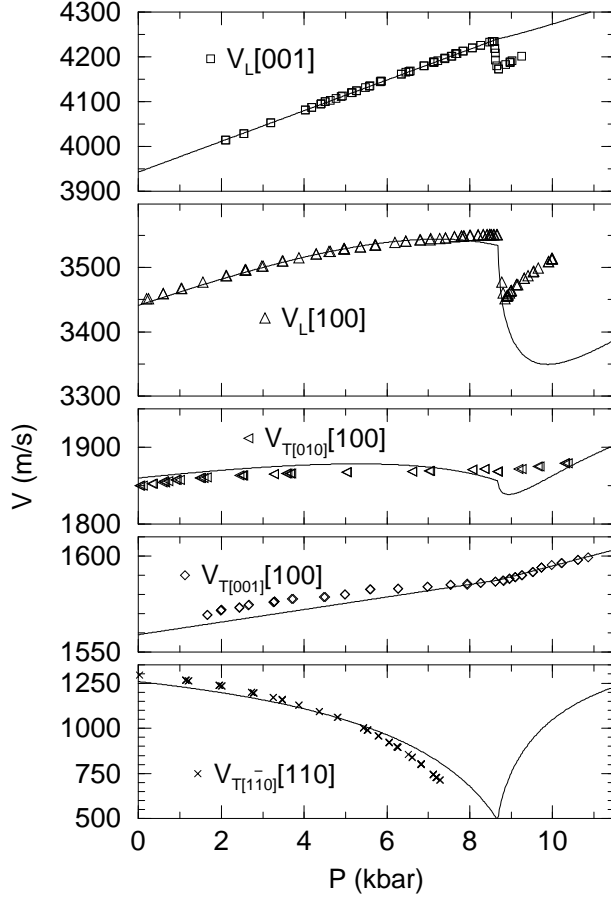


FIG. 2: Pressure dependence of the sound velocity of longitudinal (L) and transversal (T) modes measured at room temperature along the principal crystallographic directions of $\text{Rb}_4\text{LiH}_3(\text{SO}_4)_4$. The experimental results are represented by open symbols while the continuous lines correspond to predictions derived from the pseudo-proper ferroelastic model presented in the Appendix.

termine what might be the influences of these domains on the measured quantities. Thus, in order to ascertain if our measurements represent the intrinsic elastic properties of $\text{Rb}_4\text{LiH}_3(\text{SO}_4)_4$, we compare in Fig. 4 the temperature dependence of the velocity of longitudinal waves propagating along two orthogonal directions in the ab plane ([100] and [010] directions). As the x and y directions are no longer equivalent in a monoclinic phase, one would expect a significant difference between these two modes. The fact that both sets of data are practically identical below T_c indicates that the size of the domains is smaller than our acoustic wavelength ($\lambda \approx 100 \mu\text{m}$) at 30 MHz. Thus, based on this comparison, it is clear that our results obtained in the ferroelastic phase, as well as those obtained by Breczewski et al.¹⁰, do not reflect the intrinsic elastic properties of $\text{Rb}_4\text{LiH}_3(\text{SO}_4)_4$. For that reason, the Landau models presented in the Appendix are tested using results obtained principally in the paraelastic phase (tetragonal phase).

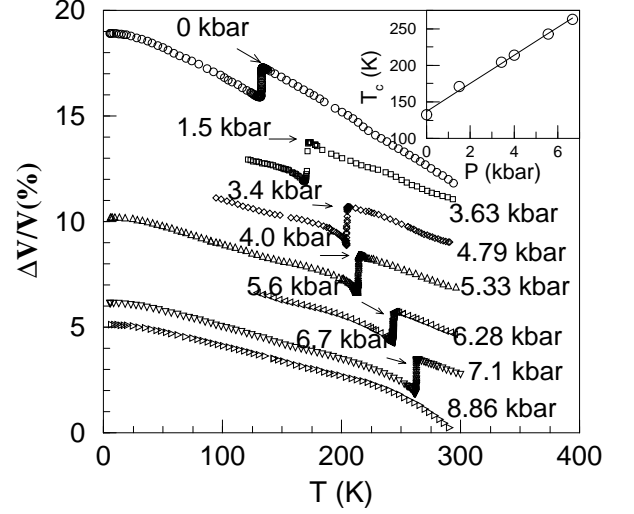


FIG. 3: Temperature dependence of the sound velocity of longitudinal waves propagating along the z -axis ($V_L[001]$) measured at different pressures. The inset shows the pressure dependence of the ferroelastic critical temperature T_c for $\text{Rb}_4\text{LiH}_3(\text{SO}_4)_4$.

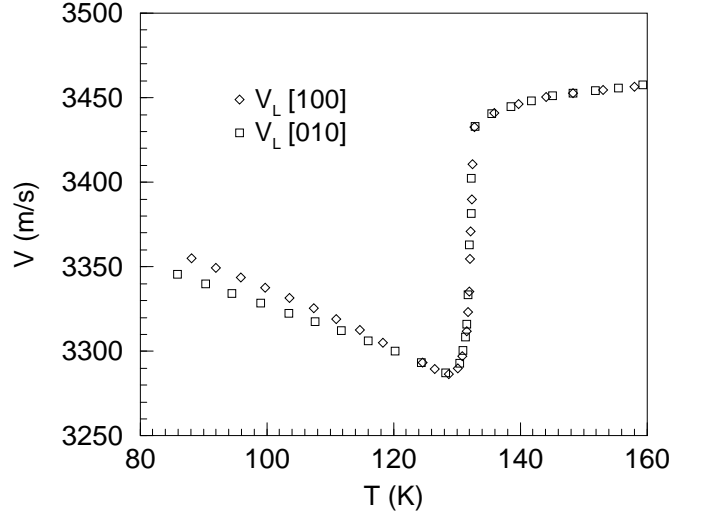


FIG. 4: Comparison of the temperature dependence of the velocity of longitudinal waves propagating along two orthogonal directions in the ab plane ([100] and [010] directions).

So far, the elastic properties of $\text{Rb}_4\text{LiH}_3(\text{SO}_4)_4$ have been qualitatively analyzed by different groups^{9,10} using two different Landau-type models. In one case, they consider that the order parameter corresponds to the strains $e_1 - e_2$ and e_6 (proper ferroelastic) while in the other scenario the order parameter is unknown but has the same symmetry as the strains mentioned previously (pseudo-ferroelastic). In this paper, we present (see Appendix) a comprehensive derivation of a proper and pseudo-proper models for a $4 \rightarrow 2$ ferroelastic phase transition. Both of these models are derived using a minimum number

of coupling factors. Our principal goal is to see if one could determine the true nature of the order parameter based on a detailed analysis of the elastic properties of $\text{Rb}_4\text{LiH}_3(\text{SO}_4)_4$.

According to both models derived in the Appendix (see Eq. 23 and Eq. 32), the elastic constants C_{11} , C_{16} , and C_{66} are expected to soften while C_{12} becomes stiffer as T_c is approached from above (or approach P_c from below). The main qualitative difference between these models is that the softening and stiffening are expected to be linear for a proper ferroelastic transition while it could be non-linear in the other case. Using the relations given in reference [10] and our high resolution velocity measurements, it is easy to determine the temperature and pressure dependence of the principal elastic constants. Considering that the value of C_{16} is an order of magnitude smaller than C_{11} ^{9,10}, we can consider, as a reasonable approximation, that the temperature and pressure dependence of C_{11} is captured by that of $V_L[100]$. Thus, our high resolution measurements indicate that C_{11} indeed softens, however, its temperature and pressure dependence are significantly non-linear. This first constatation is reinforced by a comparison of the velocity measurements performed on $\text{Rb}_4\text{LiH}_3(\text{SO}_4)_4$ and the isomorphous compound $\text{K}_4\text{LiH}_3(\text{SO}_4)_4$. As $\text{K}_4\text{LiH}_3(\text{SO}_4)_4$ shows no ferroelastic transition⁹, it can be used to accurately determined the anharmonic temperature dependence of the elastic constants in the absence of softening due to the transition. As an example, we compare in Fig. 5 the results obtained for longitudinal modes propagating along the z and x directions. Along the z -direction, we note that both compounds have the same absolute velocity at room temperature and exhibit the same temperature dependence. This is consistent with both models as no influence of the soft mode is expected on C_{33} in the para-elastic phase. Along the x -direction, the comparison of $V_L[100]$ for these two compounds indicates that the contribution associated with the soft mode is indeed non-linear and thus more compatible with the pseudo-ferroelastic description.

So far, our qualitative observations seem to indicate that the elastic properties of $\text{Rb}_4\text{LiH}_3(\text{SO}_4)_4$ are more consistent with the predictions based on pseudo-ferroelastic model. A more rigorous test can be performed by carrying on a detailed numerical comparison using the prediction giving in the Appendix. While the elastic constants are determined by sound velocity measurements realized at room temperature, the magnitude of the coupling terms, as well as α and A_4 , need to be determined independently. Moreover, it is also important to determine the anharmonic contributions which are independent of the transition. In the case of $\text{Rb}_4\text{LiH}_3(\text{SO}_4)_4$, these contributions have been determined from velocity measurements performed on the isomorphous compound $\text{K}_4\text{LiH}_3(\text{SO}_4)_4$. Finally, let mention that both models include only eight adjustable parameters and that six of them are determined independently using the temperature dependence of the strains,

the pressure dependence of T_c ($dT_c/dP = 19.1$ K/kbar), and the normalization of the order parameter. The last two parameters ζ and η , which only influence C_{44} and C_{45} , can be set manually. To illustrate how stringent this process is, we present in Fig. 6 the predictions based on Eqs. 9 -14 and the temperature dependence of the strains obtained from high-resolution neutron diffraction results published by Mróz et al.⁸ As $e_1 - e_2$ and e_6 show a well defined mean field temperature dependence, we can safely assume that the neutron data reflect the microscopic properties within the macroscopic domains in the ferroelastic phase. When all adjustable parameters are determined, we then calculate the velocities along different directions by solving the Christoffel's equation using the elastic tensors Eq. 23 and Eq. 32 for the pseudo-proper and proper ferroelastic transition, respectively. The results of the calculations (continuous line) based on the pseudo-proper model are presented in Fig. 1-2 along with the experimental data points. In the para-elastic phase, the agreement between the prediction of the pseudo-proper model and experimental results, as a function of temperature and

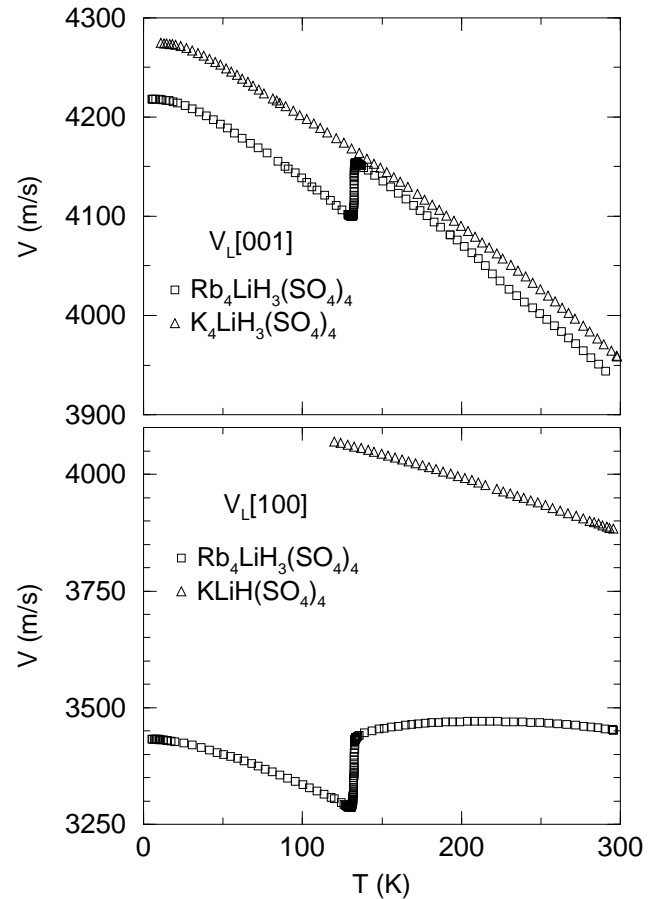


FIG. 5: Comparison of the elastic properties of $\text{Rb}_4\text{LiH}_3(\text{SO}_4)_4$ and the isomorphous compound $\text{K}_4\text{LiH}_3(\text{SO}_4)_4$ using the temperature dependence of $V_L[100]$ and $V_L[001]$.

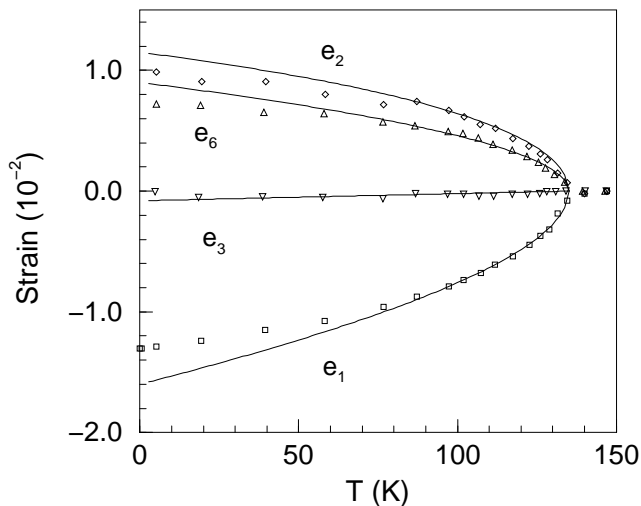


FIG. 6: Temperature dependence of the spontaneous strains. The points correspond to results obtained from Mróz et al.⁸ while the continuous line are calculated using Eq. 9 -14.

pressure, is quite remarkable (within of percent). Naturally, the agreement in the ferroelastic phase is not as good considering that the elastic properties are significantly affected by the existence of structural domains below T_c . As an ultimate test, we compare in Fig. 7 the predictions of the proper model (dash line) and the pseudo-proper model (continuous line) relative to experimental data showing the largest variation. These variations are obtained using transverse modes propagating in the xy plane at an angle ϕ relative to the [110] direction (with $\phi = +5^\circ, 0^\circ, -10^\circ$) with its polarization in the xy plane. From that comparison, it is clear that we systematically obtain a better agreement with the pseudo-proper model rather than the proper ferroelastic model. In Fig. 7 we have limited our comparison to $V_{T[110]}[110]$, however, we reach the same conclusion using results obtained for $V_L[100]$.

V. SOFT MODE

The data presented in Fig. 7 also confirms a larger softening as the direction of propagation, for transverse mode polarized in the xy plane, is a few degrees away from the [110] direction (approximately -10° relative to the [110]

direction). This observation complies with previous Brillouin scattering measurements⁹ which show less softening as the direction of propagation is changed toward [010] instead of [100]. However, in their data analysis, they also claim that $\text{Rb}_4\text{LiH}_3(\text{SO}_4)_4$ shows incomplete softening at T_c , a claim that we revisit in this section. The effective modulus for the soft acoustic mode of a $4 \rightarrow 2$ ferroelastic phase transition can be obtained by finding the eigenvalues of the submatrix corresponding to the

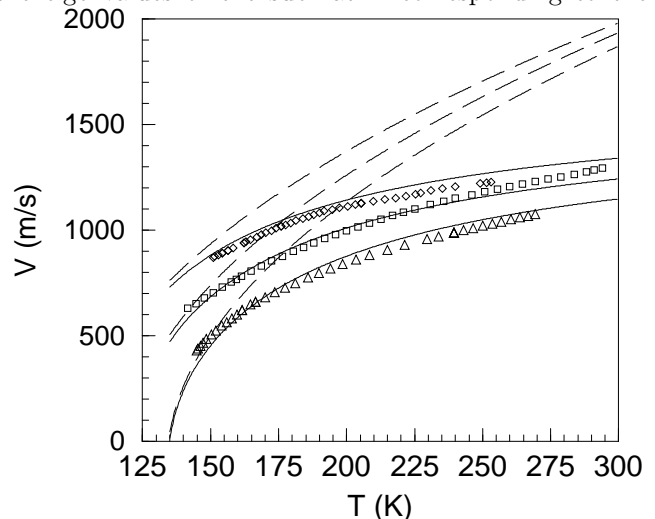


FIG. 7: Temperature dependence of the velocity of transverse waves polarized in the xy plane and propagating along different directions in the xy plane ($\phi = +5^\circ, 0^\circ$, and -10° relative to the [110] direction). Here, the continuous and dash lines correspond to predictions based on a pseudo and proper ferroelastic models presented in the Appendix.

strain components $e_1 - e_2$ and e_6 ,

$$\begin{pmatrix} \frac{C_{11}-C_{12}}{2} & C_{16} \\ C_{16} & C_{66} \end{pmatrix}. \quad (1)$$

We would like to point out that the submatrix used here differs from the one published by Boccara¹³. Considering that elastic tensors must be symmetric, it is obvious that some of the results found in Boccara¹³ are inexact and that they correspond to simple topographic errors. Thus, contrary to the expression used by Mroz et al.⁹, which was derived from expressions found in Boccara¹³, the appropriate relation for the soft modulus is

$$C_{soft} = \frac{1}{2} \left(\frac{C_{11}-C_{12}}{2} + C_{66} - \sqrt{\left(\frac{C_{11}-C_{12}}{2} - C_{66} \right)^2 + 4C_{16}^2} \right) \quad (2)$$

while the associated direction of propagation¹⁴ is given by

where the angle ϕ is defined relative the [110] direction. Using the measured elastic constants of $\text{Rb}_4\text{LiH}_3(\text{SO}_4)_4$

at room temperature, the expected direction for the soft mode should correspond to $\phi \cong -13^\circ$. This prediction ($45^\circ + \phi = 32^\circ$ relative to the x-axis) agrees well with the orientations of the domain walls observed in the ferroelastic phase⁸. As that direction does not coincide with any of the principal crystallographic directions, this has contributed to delay the experimental determination of the actual soft mode in $\text{Rb}_4\text{LiH}_3(\text{SO}_4)_4$. According to our recent investigation, the data obtained at $\phi = -10^\circ$ indicate a larger variation relative to the results obtained at $\phi = 0^\circ$, which is very consistent with the numerical prediction. Unfortunately, due to a rapid increases in the acoustic attenuation close to T_c , we were not able to perform the measurement down to T_c . Nevertheless, considering that the theoretical prediction based on the pseudo ferroelastic model agree well with our experimental data, we believe that within the experimental uncertainties there is no strong evidence of incomplete softening in $\text{Rb}_4\text{LiH}_3(\text{SO}_4)_4$. Thus, it is clear, based on the results presented in this section, that the conclusion reached by Mroz et al.⁹ is inexact.

VI. CONCLUSIONS

In this investigation, we have presented a detailed analysis of the elastic properties of $\text{Rb}_4\text{LiH}_3(\text{SO}_4)_4$. A substantial set of experimental data, obtained as a function of temperature and pressure, is compared to two Landau models associated with a $4 \rightarrow 2$ ferroelastic phase transition. The possible scenarios considered here correspond to the proper ferroelastic case where the instability is driven by the strains while in the pseudo-proper situation the order parameter is unknown. In the later case, even the order parameter is unknown, its symmetry must be identical to the order parameter defined for the proper ferroelastic case. Both models are derived using a minimum number of coupling parameters which are adjusted from thermal expansion data⁸ and the pressure dependence of the critical temperature $dT_c/dP = 19.1 \pm 0.2 \text{ K/kbar}$ obtained in this work. Our analysis clearly shows that within the frame work of the pseudo-proper ferroelastic model, it is possible to obtain predictions that are simultaneously consistent with the temperature and pressure dependence of the elastic constants, the pressure dependence of T_c and thermal expansion. No such quantitative agreement is obtained using the proper ferroelastic model. Thus, as suggested by our investigation, $\text{Rb}_4\text{LiH}_3(\text{SO}_4)_4$ should be considered as a pseudo-proper ferroelastic compound. If our conclusion is accurate, this implies that the nature of the order parameter, driving the ferroelastic transition in $\text{Rb}_4\text{LiH}_3(\text{SO}_4)_4$, is still unknown. So far, there has been a limited number of Raman scattering measurements on $\text{Rb}_4\text{LiH}_3(\text{SO}_4)_4$ ¹⁵. However, even if they observed a soft optical B mode, the authors of Ref. 15 claim that the variation of that particular mode is insufficient to account for the transition. It is worthwhile to note that,

in the presence of linear coupling between acoustical and optical modes¹², while the actual transition takes place at T_c , the extrapolated temperature dependence of the soft optical energy in the paraelastic phase is expected to vanish at a temperature T_o . Based on our numerical predictions, T_o is approximately equal to 20 K in the case of $\text{Rb}_4\text{LiH}_3(\text{SO}_4)_4$. We believe that further investigations are certainly necessary in order to clarify the nature of the actual mode responsible for the ferroelastic transition in $\text{Rb}_4\text{LiH}_3(\text{SO}_4)_4$.

Finally, as we have clearly demonstrated in this paper, there is no strong experimental evidence that $\text{Rb}_4\text{LiH}_3(\text{SO}_4)_4$ show incomplete softening of the soft elastic constant at T_c . Consequently, the ferroelastic character of $\text{Rb}_4\text{LiH}_3(\text{SO}_4)_4$ is not necessarily unique, for example, its properties seem very similar to those of $(\text{NH}_4)_4\text{LiH}_3(\text{SO}_4)_4$ which shows a $4 \rightarrow 2$ ferroelastic phase transition at 236 K¹⁶. It would be interesting to use a similar numerical analysis in order to determine the nature of that ferroelastic transition.

VII. APPENDIX

A. Landau Models

The direct group-subgroup relationship for the $4 \rightarrow 2$ ferroelastic phase transition imposes that the spontaneous strain¹¹ associated with this transition must correspond to the combination $\alpha_1 (e_1 - e_2) + \alpha_6 e_6$. This effective strain can then act as the principal order parameter (proper ferroelastic transition) or couple bilinearly to the order parameter Q. In the later case, the order parameter Q could correspond to the softening of an optical phonon and the phase transformation is then referred to as a pseudoproper ferroelastic transition¹¹. Even if there is no direct evidence of a soft optical mode in $\text{Rb}_4\text{LiH}_3(\text{SO}_4)_4$ ¹⁵, this later scenario should not be dismissed. As we show in this paper, these two types of ferroelastic transition should in principle produce subtle differences in the elastic properties of $\text{Rb}_4\text{LiH}_3(\text{SO}_4)_4$. The predictions, derived from the models presented in the next section, are then compared to our experimental data in order to determine whether $\text{Rb}_4\text{LiH}_3(\text{SO}_4)_4$ should be regarded as a proper or pseudo-proper ferroelastic compound.

B. Pseudo-proper Ferroelastic Model

Considering that we are particularly interested in the pressure and temperature dependence of the elastic properties, we express the Gibbs free energy into four distinct contributions such as

$$G(Q, e_i) = F_L(Q) + F_{el}(e_i) + F_c(Q, e_i) + F_P(P, e_i) . \quad (4)$$

Here, $F_L(Q)$ is the usual second-order Landau-type free energy in terms of an order parameter Q ,

$$F_L(Q) = \frac{1}{2} A_2 Q^2 + \frac{1}{4} A_4 Q^4 \quad (5)$$

where $A_2 = \alpha (T - T_o)$ depends explicitly on temperature while the pressure contribution is introduced in $F_P(P, e_i)$ of Eq. 4. In the presence of external stresses σ_i , this contribution is normally written as $-\sum_i \sigma_i e_i$. In the case of an hydrostatic pressure P the stress associated with longitudinal strains ($i = 1, 2, 3$) corresponds to $\sigma_i = -P$ while for shear strains $\sigma_j = 0$ ($j = 4, 5, 6$), hence

$$F_P(P, e_i) = P (e_1 + e_2 + e_3). \quad (6)$$

This contribution is crucial in order to calculate the pressure dependence of the elastic constants as well as to determine the pressure dependence of the critical temperature. Furthermore, this is achieved without adding any additional adjustable parameters. The elastic energy

$F_{el}(e_i)$ is also straightforward to derive as it is imposed by the symmetry of the high temperature phase. Thus, for a point group 4 symmetry¹⁴

$$\begin{aligned} F_{el}(e_i) = & \frac{1}{2} C_{11} (e_1^2 + e_2^2) + \frac{1}{2} C_{33} e_3^2 + \frac{1}{2} C_{44} (e_4^2 + e_5^2) \\ & + \frac{1}{2} C_{66} e_6^2 + C_{12} e_1 e_2 + C_{13} (e_1 + e_2) e_3 \\ & + C_{16} (e_1 - e_2) e_6 \end{aligned} \quad (7)$$

where C_{ik} represent the bare elastic constants at high temperatures. Finally, the most critical term corresponds to the coupling energy $F_c(Q, e_i)$ which takes into account the coupling between the strain components e_i and the order parameter Q . For a $4 \rightarrow 2$ pseudo-proper ferroelastic transition, we know that the order parameter Q must transform as the spontaneous strain $\alpha_1(e_1 - e_2) + \alpha_6 e_6$ under the symmetry operations of the high temperature phase. Thus, using fundamental symmetry arguments, the coupling terms considered in this paper are

$$F_c(Q, e_i) = \beta Q (e_1 - e_2) + \gamma Q e_6 + \delta Q^2 e_3 + \lambda Q^2 (e_1 + e_2) + \zeta e_4 e_5 Q + \eta (e_4^2 + e_5^2) Q^2 \quad (8)$$

Here, we only consider terms which are fully compatible with a $4 \rightarrow 2$ structural transformation. The Gibbs energy, as defined in this paper (Eq. 4-8), gives a phenomenological framework which can now be used in order to derive the elastic properties of a $4 \rightarrow 2$ pseudo-proper ferroelastic compound. From the minimization of the Gibbs energy with respect to e_i , we obtain a series of expressions for the spontaneous strains $e_i(Q)$. At ambient pressure these relations correspond to

$$e_1 - e_2 = \frac{2 (\gamma C_{16} - \beta C_{66})}{(C_{11} - C_{12}) C_{66} - 2 C_{16}^2} Q \quad (9)$$

$$e_1 + e_2 = \frac{2 (\delta C_{13} - \lambda C_{33})}{(C_{11} + C_{12}) C_{33} - 2 C_{13}^2} Q^2 \quad (10)$$

$$e_3 = -\frac{(\delta (C_{11} + C_{12}) - 2 \lambda C_{13})}{(C_{11} + C_{12}) C_{33} - 2 C_{13}^2} Q^2 \quad (11)$$

$$e_4 = 0 \quad (12)$$

$$e_5 = 0 \quad (13)$$

$$e_6 = -\frac{\gamma (C_{11} - C_{12}) - 2 \beta C_{16}}{(C_{11} - C_{12}) C_{66} - 2 C_{16}^2} Q \quad (14)$$

As $(e_1 - e_2)$ and e_6 display the same symmetry characteristic as Q , it is then natural to find that they are proportional to Q . We also obtain that $e_4 = e_5 = 0$ which is again compatible with a $4 \rightarrow 2$ symmetry change. Furthermore, using the minimization with respect to the order parameter Q , the corresponding expressions for the order parameter Q , the critical temperature T_c and its pressure dependence can be written as

$$Q(T, P) = \sqrt{\frac{\alpha C_a (T_c + \frac{dT_c}{dP} P - T)}{\Delta}} \quad (15)$$

$$T_c = T_o - \frac{C_b}{\alpha C_a} \quad (16)$$

$$\frac{dT_c}{dP} = 2 \frac{C_c}{\alpha C_a} \quad (17)$$

where

$$C_a = (C_{11} + C_{12}) C_{33} - 2 C_{13}^2 \quad (18)$$

$$C_b = \gamma^2 (C_{11} - C_{12}) + 2\beta (\beta C_{66} - 2\gamma C_{16}) \quad (19)$$

$$C_c = \delta (C_{11} + C_{12} - 2 C_{13}) + 2\lambda (C_{33} - C_{13}) \quad (20)$$

$$\Delta = 8\delta\lambda C_{13} - 2A_4 C_{13}^2 - 4\lambda^2 C_{33} + C_{11}(A_4 C_{33} - 2\delta^2) + C_{12}(A_4 C_{33} - 2\delta^2) \quad (21)$$

Finally, the elastic constants are calculated using¹⁷

$$C_{mn}^* = \frac{\partial^2 F}{\partial e_m \partial e_n} - \frac{\partial^2 F}{\partial Q \partial e_m} \left(\frac{\partial^2 F}{\partial Q^2} \right)^{-1} \frac{\partial^2 F}{\partial e_n \partial Q}. \quad (22)$$

According to this model, the elastic tensor associated with the tetragonal 4 phase is

$$\begin{pmatrix} C_{11} - \frac{\beta^2}{A(T,P)} & C_{12} + \frac{\beta^2}{A(T,P)} & C_{13} & 0 & 0 & C_{16} - \frac{\beta\gamma}{A(T,P)} \\ C_{12} + \frac{\beta^2}{A(T,P)} & C_{11} - \frac{\beta^2}{A(T,P)} & C_{13} & 0 & 0 & -C_{16} + \frac{\beta\gamma}{A(T,P)} \\ C_{13} & C_{13} & C_{33} & 0 & 0 & 0 \\ 0 & 0 & 0 & C_{44} & 0 & 0 \\ 0 & 0 & 0 & 0 & C_{44} & 0 \\ C_{16} - \frac{\beta\gamma}{A(T,P)} & -C_{16} + \frac{\beta\gamma}{A(T,P)} & 0 & 0 & 0 & C_{66} - \frac{\gamma^2}{A(T,P)} \end{pmatrix} \quad (23)$$

while the corresponding tensor for the monoclinic 2 phase is

$$\begin{pmatrix} C_{11} - \frac{X_{Q+}^2}{Y_Q} & C_{12} + \frac{X_{Q+}X_{Q-}}{Y_Q} & C_{13} - \frac{2\lambda Q X_{Q+}}{Y_Q} & 0 & 0 & C_{16} - \frac{\gamma X_{Q+}}{Y_Q} \\ C_{12} + \frac{X_{Q+}X_{Q-}}{Y_Q} & C_{11} - \frac{X_{Q-}^2}{Y_Q} & C_{13} + \frac{2\lambda Q X_{Q-}}{Y_Q} & 0 & 0 & -C_{16} + \frac{\gamma X_{Q-}}{Y_Q} \\ C_{13} - \frac{2\lambda Q X_{Q+}}{Y_Q} & C_{13} + \frac{2\lambda Q X_{Q-}}{Y_Q} & C_{33} - \frac{4\delta^2 Q^2}{Y_Q} & 0 & 0 & -\frac{2\gamma\delta Q}{Y_Q} \\ 0 & 0 & 0 & C_{44} + 2\eta Q^2 & \zeta Q & 0 \\ 0 & 0 & 0 & \zeta Q & C_{44} + 2\eta Q^2 & 0 \\ C_{16} - \frac{\gamma X_{Q+}}{Y_Q} & -C_{16} + \frac{\gamma X_{Q-}}{Y_Q} & -\frac{2\gamma\delta Q}{Y_Q} & 0 & 0 & C_{66} - \frac{\gamma^2}{Y_Q} \end{pmatrix} \quad (24)$$

with

$$A(T, P) = \alpha \left(T - T_o - \frac{dT_c}{dP} P \right) \quad (25)$$

$$X_{Q+} = \beta + 2\lambda Q \quad (26)$$

$$X_{Q-} = \beta - 2\lambda Q \quad (27)$$

$$Y_Q = 2A_4 Q^2 - \frac{\gamma^2(C_{11} - C_{12}) - 2\beta^2 C_{66}}{(C_{11} - C_{12})C_{66} - 2C_{16}^2}. \quad (28)$$

A rapid inspection of the elastic tensor, corresponding to the solution below T_c (or above P_c), indicates that its form is consistent with the elastic tensor of the monoclinic class 2. This indicates that the coupling terms considered in the Gibbs energy includes all terms which are fully compatible with a $4 \rightarrow 2$ symmetry change.

ergy, the Landau energy, and the elastic energy as defined in Eq. 4 - Eq. 5, and Eq. 7, respectively. The main difference being that the order parameter Q now corresponds to a strain combination defined as $Q = \alpha_1(e_1 - e_2) + \alpha_6 e_6$. Thus, the coupling terms invariant with respect to the high temperature symmetry are

C. Proper Ferroelastic Model

In the case of a proper ferroelastic model, the derivation is slightly different. We can still write the Gibbs en-

$$F_c(e_i) = \delta Q^2 e_3 + \lambda Q^2 (e_1 + e_2) + \zeta e_4 e_5 Q + \eta (e_4^2 + e_5^2) Q^2 \quad (29)$$

Using the minimization of the Gibbs energy with respect to e_i , the solutions for $e_1 + e_2$, e_3 , e_4 , e_5 , dT_c/dP remain identical to those obtained for the pseudo-proper case while

$$T_c = T_o - \frac{-2C_{16}^2 + (C_{11} - C_{12})C_{66}}{\alpha(\alpha_6^2(C_{11} - C_{12}) + 2\alpha_1(\alpha_1 C_{66} - 2\alpha_6 C_{16}))}. \quad (30)$$

Finally, as that the Gibbs energy is now only a function of strains, the elastic constants are directly obtained using

$$C_{mn}^* = \frac{\partial^2 F}{\partial e_m \partial e_n} . \quad (31)$$

Thus, in the case a $4 \rightarrow 2$ proper ferroelastic transition, the elastic tensor for the paraelastic phase is given by

$$\begin{pmatrix} C_{11} + \alpha_1^2 A(T, P) & C_{12} - \alpha_1^2 A(T, P) & C_{13} & 0 & 0 & C_{16} + \alpha_1 \alpha_6 A(T, P) \\ C_{12} - \alpha_1^2 A(T, P) & C_{11} + \alpha_1^2 A(T, P) & C_{13} & 0 & 0 & -C_{16} - \alpha_1 \alpha_6 A(T, P) \\ C_{13} & C_{13} & C_{33} & 0 & 0 & 0 \\ 0 & 0 & 0 & C_{44} & 0 & 0 \\ 0 & 0 & 0 & 0 & C_{44} & 0 \\ C_{16} + \alpha_1 \alpha_6 A(T, P) & -C_{16} - \alpha_1 \alpha_6 A(T, P) & 0 & 0 & 0 & C_{66} + \alpha_6^2 A(T, P) \end{pmatrix} \quad (32)$$

where $A(T, P) = \alpha (T - T_c - \frac{dT_c}{dP}P)$. Thus, the temperature and pressure dependence of the elastic constants should be linear. This differs from the pseudo-proper model where the variation in the elastic constants is expected to be inversely proportional to $A(T, P)$. Naturally, depending on the strength of the coupling parameters this dependence could be quasi-linear. Thus, a clearly distinction between these two models can only be obtained through a detailed comparison with experimental results.

VIII. ACKNOWLEDGMENTS

This work was supported by grants from the Natural Science and Engineering Research Council of Canada (NSERC), Canada Foundation for Innovation (CFI) as well as by the Ministry of Education and Science (Poland), Grant No. 1 PO3B 066 30.

-
- ¹ B. Mróz, H. Kiefte, and M. J. Clouter, *Ferroelectrics* **82**, 105 (1988).
 - ² B. Mróz, J. A. Tuszynski, H. Kiefte, and M. J. Clouter, *J. Phys.: Condens. Matter* **1**, 4425 (1989).
 - ³ T. Wolejko, P. Piskunowicz, T. Brezewski, and T. Krajewski, *Ferroelectrics* **81**, 175 (1988).
 - ⁴ T. Wolejko, G. Pakulski, and Z. Tylczynski, *Ferroelectrics* **81**, 179 (1988).
 - ⁵ P. Piskunowicz, T. Brezewski, and T. Wolejko, *Phys. Stat. sol. (a)* **114**, 505 (1989).
 - ⁶ J. Mingé and T. Krajewski, *Phys. Stat. Sol. (a)* **109**, 193 (1988).
 - ⁷ A. Pietraszko and K. Lukaszewicz, *Z. Krystallogr.* **185**, 564 (1988).
 - ⁸ B. Mróz, S. M. Kim, B. M. Powell, H. Kiefte, and R. L. Donabarger, *Phys. Rev. B* **55**, 11174 (1997).

- ⁹ B. Mróz, H. Kiefte, M. J. Clouter, and J. A. Tuszynski, *J. Phys.: Condens. Matter* **3**, 5673 (1991).
- ¹⁰ T. Brezewski, A. Gomez-Cuevas, J. M. Perez-Mato, and E. H. Bocanegra, *Solid State Commun.* **76**, 639 (1990).
- ¹¹ P. Tolédano, M. M. Fejer, and B. A. Auld, *Phys. Rev. B* **27**, 5717 (1983).
- ¹² A. Pinczuk, G. Burns, and F. H. Dacol, *Solid State Commun.* **24**, 163 (1977).
- ¹³ N. Boccara, *Ann. of Phys.* **47**, 40 (1968).
- ¹⁴ E. Dieulesaint and D. Royer, *Elastic Waves in Solids* (John Wiley and Sons Ltd., 1980).
- ¹⁵ B. Mroz, M. Kaczmarzski, H. Kiefte, and M. J. Clouter, *J. Phys.: Condens. Matter* **4**, 7515 (1992).
- ¹⁶ B. Mróz, H. Kiefte, M. J. Clouter, and J. A. Tuszynski, *J. Phys.: Condens. Matter* **5**, 6377 (1993).
- ¹⁷ W. Rehwal, *Adv. Phys.* **22**, 721 (1973).